# Smoothing effect of sensitivity map on fMRI data using a novel regularized self-calibrated estimation method

**Y. Kim[1], J. A. Fessler[2], and D. C. Noll[1]**

[1]Biomedical Engineering, University of Michigan, Ann Arbor, MI, United States, [2]Electrical Engineering and Computer Science department, University of Michigan, Ann Arbor, MI, United States

## Introduction

Applying parallel imaging technique, such as SENSE [1], to functional MRI can help to overcome the limitations of current fMRI techniques by increasing the spatiotemporal resolution or by reducing the susceptibility artifacts at the expense of image domain SNR. In dealing with time series fMRI data, TSENSE [2] can be used to make efficient use of time and k-space. Like other image-domain based parallel imaging techniques, the performance of TSENSE heavily relies on the accuracy of the sensitivity maps that are necessary for the unaliasing process. Thus, accurate estimation of sensitivity maps is particularly important. In TSENSE, both spatial smoothing and temporal smoothing are applied to the sensitivity maps to improve robustness to noise. However, the effect of smoothing has not been thoroughly investigated to date. In our study, we investigate the effects of sensitivity map smoothing on motion corrupted fMRI data. We also propose a novel self-calibrated sensitivity map estimation technique that controls noise and smoothness via regularization.

## Methods

In dynamic parallel imaging techniques with time-interleaved acquisition schemes, such as TSENSE, we can combine under-sampled neighboring time point data to produce fully-sampled k-space data set. In our experiment, we acquired spiral data with a reduction factor of 2. Thus, two neighboring time points were combined to form one fully sampled k-space data. Denoting the fully sampled image for each coil $l$ as $z_l$ and the reference image as $z_{ref}$, we can estimate $l$-th coil sensitivity map, $s_l$ via

$$\hat{s}_l \triangleq \arg\min_s \frac{1}{2}\left\| z_l - diag\{z_{ref}\}s \right\|^2 + \beta R(s)$$

where $\beta R(s)$ is a spatial roughness penalty function. The reference image, $z_{ref}$, can be obtained by taking the sum-of-squares [1], or geometric mean [3] of the individual coil images. The phase of one coil's image can further be incorporated into this term to prevent inclusion of the underlying object's phase in the sensitivity map. Using this approach, we improve robustness to noise in regions with low signal intensity and near edges since the direct division is avoided. Smoothness of the estimated sensitivity map is easily controlled by varying $\beta$.

We collected functional data on a 3T GE scanner with an 8-channel head array coil. Imaging parameters were TR = 2s, TE = 25ms, 64×64 matrix size, FOV = 22cm, 5-mm thick axial slices, and two-shot gradient echo spiral-out acquisition. During the scan, the subject was instructed to move his head right or left in response to the position of a visual cue on the screen. We acquired a total of 40 time points of undersampled data with a reduction factor of 2.

To see the effects of spatial smoothing, sensitivity maps were estimated with different smoothness factors by varying $\beta$. We expect this spatial smoothing to mitigate problems with noise around the edges of the sensitivity maps. We also examined the effects of temporal averaging of sensitivity maps by changing the number of neighboring time points used for moving averages. This temporal smoothing could potentially deal with inconsistencies in the estimated sensitivity maps due to motion. Estimated sensitivity maps were then applied to iterative SENSE reconstruction with CG algorithm [4] with 17 iterations. As proposed in the original TSENSE method, UNFOLD [5] was also used to remove the high frequency artifacts created by alternating interleaves. Temporal SNR (TSNR) and image domain error were used as metrics for comparing the results.

## Results

In Figure 1(a), the magnitude of the mean (top) and variance (bottom) of complex sensitivity map over time is shown. Time course of two voxels of sensitivity map, one at the center(blue) and the other one close to the edge(red), are plotted in Figure 1(b). Absolute value of coefficient of variation (=σ/μ) a.k.a. CV, are also calculated for each voxel and are shown in Figure 1(b). Sensitivity values within the object do not vary much over time compared to those close to the periphery. In Figure 2, effect of spatial smoothing of sensitivity map is shown in terms of image domain error [%] and TSNR [dB]. Appropriate spatial smoothing reduces image domain error and increases the TSNR. In Figure 3, we can see that image domain error decreases and TSNR increases with the number of neighboring time points used for moving average.

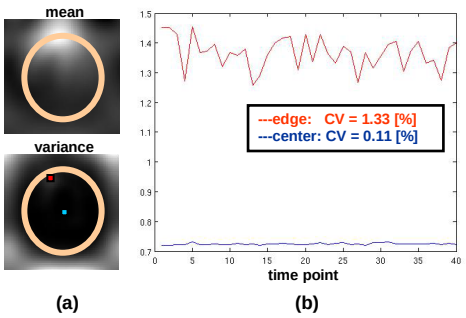


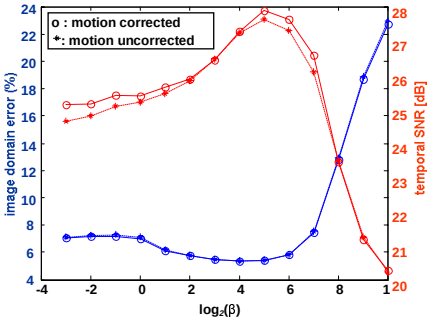


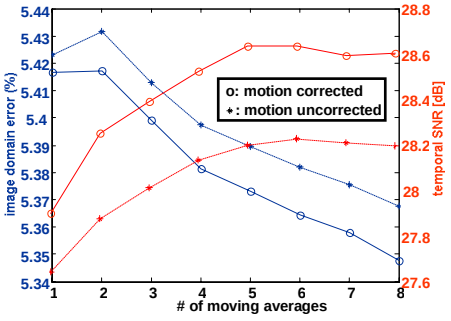


**Figure 1** (a) Mean (top) and variance (bottom) of complex sensitivity profile over total time point. (b) time course of sensitivity map at the center (blue) and at around the edges (red) of the head

**Figure 2** Effect of spatial smoothing on sensitivity maps measured as image domain error [%] and TSNR [dB]

**Figure 3** Effect of temporal smoothing of sensitivity map measure as image domain error [%] and TSNR [dB]

## Discussion

In this study, we investigated the effects of spatial and temporal smoothing of sensitivity maps for motion corrupted fMRI data. Spatial smoothing of sensitivity maps reduces image domain error and improves TSNR. However, over-smoothing ($\log_2(\beta)>7$) largely degrades both performance metrics. This suggests that we can find the good sensitivity map by adjusting the smoothness of sensitivity maps. In further study, we will investigate how to choose $\beta$ to have a good estimate of sensitivity map. We can also conclude that temporal smoothing of sensitivity map via a sliding window technique helps to improve both performance metrics. However, we limit this conclusion to fMRI data since the sliding window technique has been shown not to be beneficial in cardiac imaging [6]

**References:** [1] Pruessmann, MRM 1999;42:952-962 [2] Kellman, MRM 2001;45:846-52 [3] Cao, Proc. ISMRM 2005, p2447. [4] Sutton, Proc. ISMRM 2001, p771 [5] Madore, MRM 1999;42:813–828 [6] Tsao, MRM 2003;50:1031–1042 **Acknowledgement:** This work is supported by NIH Grants EB002683